

InF-ATPG: Intelligent FFR-Driven ATPG with Advanced Circuit Representation Guided Reinforcement Learning

Bin Sun^{1,2}, Rengang Zhang^{1,2}, Zhiteng Chao^{1,2,3}, Zizhen Liu^{*1,2}, Jianan Mu^{*1,2}, Jing Ye^{1,2,3}, Huawei Li^{*1,2,3}

¹State Key Lab of Processors, Institute of Computing Technology, Chinese Academy of Sciences

²University of Chinese Academy of Sciences

³CASTEST Co., Ltd.

sunbin23@mails.ucas.ac.cn, zhangrengang23z@ict.ac.cn,
{chaozhiteng20g, liuzizhen, mujianan, yejing, lihuawei}@ict.ac.cn

Abstract—Automatic test pattern generation (ATPG) is a crucial process in integrated circuit (IC) design and testing, responsible for efficiently generating test patterns. As semiconductor technology progresses, traditional ATPG struggles with long execution times to achieve the expected fault coverage, which impacts the time-to-market of chips. Recent machine learning techniques, like reinforcement learning (RL) and graph neural networks (GNNs), show promise but face issues such as reward delay in RL models and inadequate circuit representation in GNN-based methods. In this paper, we propose InF-ATPG, an intelligent FFR-driven ATPG framework that overcomes these challenges by using advanced circuit representation to guide RL. By partitioning circuits into fanout-free regions (FFRs) and incorporating ATPG-specific features into a novel QGNN architecture, InF-ATPG enhances test pattern generation efficiency. Experimental results show InF-ATPG reduces backtracks by 55.06% on average compared to traditional methods and 38.31% compared to the machine learning approach, while also improving fault coverage.

I. INTRODUCTION

Automatic test pattern generation (ATPG) is crucial for integrated circuit (IC) testing and design for test (DFT), tasked with generating efficient test patterns to achieve high fault coverage [1], [2]. As semiconductor technology advances into deep submicron processes, the complexity of chip design has increased significantly [3], [4], making the generation of test patterns that meet fault coverage requirements increasingly time-consuming [5]. It is indicated that generating test patterns with sufficient fault coverage can take over 20% of development time, often exceeding a month [6]. Therefore, optimizing ATPG algorithms has become a pressing challenge [7], [8].

ATPG is a highly complex problem of finding signal assignments in the circuit space to satisfy specific constraints [9]. While traditional methods rely on heuristic algorithms, recent advancements introduced learning-based models aimed at enhancing searching capabilities through accumulated data rather than relying on human-driven optimization. However, these intelligent models still face problems in decision-making and representation for ATPG tasks. One major problem is delayed rewards: SmartATPG [10] uses reinforcement learning (RL) to make decisions gate-by-gate, as illustrated in Fig. 1(a). As the bandwidth and depth of the circuit increase, the fault support regions expand considerably, resulting in excessively long decision chains for gate-by-gate approaches. This elon-

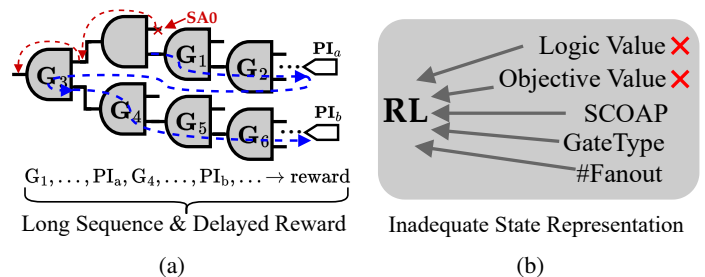


Fig. 1 Challenges in existing methods: (a) Long decision sequences lead to delayed rewards; (b) Inadequate circuit state representation for ATPG.

gation leads to delayed rewards and slow convergence in the optimization process. Another key problem is the inadequate representation of decision values, where existing approaches like FGNN2 [11] and DeepGate2 [12] leverage graph neural networks (GNNs) to model circuit functionality and structure but fail to capture ATPG-specific features like logic states and SCOAP controllability/observability [13]. These logic states play a crucial role in ATPG algorithm decision-making, as illustrated in Fig. 1(b). Thus, the main challenge for intelligent ATPG is how to efficiently represent circuits, including appropriate partitioning and state representation, to optimize RL decision-making and ensure critical ATPG-specific information is captured.

To this end, we propose InF-ATPG, an intelligent RL-based framework designed for efficient decision-making and representation in ATPG tasks. To enhance model performance, we extract broader circuit information by partitioning circuits into fanout-free regions (FFRs) [14], which reduces decision sequence length and captures higher-level structural insights. This abstraction integrates ATPG-specific features like logic states and SCOAP controllability/observability [13], providing a more accurate representation of circuit states. Since simple GNNs struggle to fully capture the complexity of logic states, we introduce the Quality-Value Graph Neural Network (QGNN), which uses a logic-value-aware multi-aggregator to model complex relationships between circuit structure and functionality. Integrating QGNN into the RL agent enhances behavior-value estimation, enabling more efficient test pattern

generation by offering deeper insight into circuit behavior. In summary, the paper makes three key contributions as follows:

- InF-ATPG innovatively explores block-level circuit spaces for RL-based ATPG. To address reward delay from long decision sequences, circuits are modeled with FFRs as the fundamental units, significantly shortening the sequence length.
- To optimize the circuit representation and tailor the RL agent for ATPG-specific tasks, InF-ATPG integrates key circuit states and features into the QGNN framework. By capturing structural and functional features more efficiently at the FFR level, QGNN drives RL agents to achieve superior training and inference performance through a logic-value-aware multi-aggregator design.
- Experimental results show that InF-ATPG reduces backtracking by an average of 55.06% compared to the traditional gate-level ATPG method, and by 38.31% compared to the existing machine learning approach. Additionally, it reduces the decision sequence length by a factor of 7.0.

II. BACKGROUND AND RELATED WORK

As the complexity of IC design increases, traditional ATPG methods face numerous challenges in handling complex circuits. Researchers have proposed various solutions to address these challenges. This section briefly reviews traditional ATPG methods, previous AI-guided methods, and their applications in ATPG.

A. Preliminary ATPG Strategies and Fanout-Free Region

ATPG. Traditional ATPG algorithms use heuristic searches to generate test patterns for fault coverage. Roth proposed D-algorithm [15] for conducting searches on circuits. Goel introduced the PODEM [16] algorithm with distance-from-primary-inputs heuristic, which significantly reduced the decision space. At the same time, Fujiwara and Shimono proposed the FAN [17] algorithm, which avoids conflicts through unique sensitization and multiple backtracing. Larrabee further improved test generation for complex circuits by introducing SAT-based solving techniques [18]–[20]. Building on this, researchers subsequently introduced heuristic optimization methods such as Simulated Annealing [21], [22], but these traditional methods still struggle with growing circuit complexity.

Fanout-Free Region. Fanout-free regions (FFRs) decompose a circuit into sub-regions in which every gate, except for the FFR head, has a single fanout, simplifying the internal dependencies of each block. This localized structure reduces decision complexity, allowing more efficient test generation by confining the search space within smaller, independent regions. It should be noted that the FAN [17] algorithm utilizes FFR. FAN avoids conflicts through reverse implications across multiple gates, making decisions at FFR roots through a voting mechanism. However, when the number of gates capable of reverse implication in the circuit is insufficient, performance degradation occurs.

B. Machine Learning Techniques

Reinforcement Learning. Reinforcement learning (RL) learns optimal policies through interaction with the environment, making it particularly suitable for tasks requiring sequential decision-making. Sutton and Barto laid the theoretical foundation for RL [23], while Watkins and Dayan’s Q-learning algorithm provided a classical approach to action selection in RL [24]. Recently, deep reinforcement learning (DRL) has combined deep neural networks with RL models, such as Mnih *et al.*’s deep Q-network (DQN) [25]. Schaul *et al.* introduced Prioritized Experience Replay (PER), improving DQN’s training efficiency and convergence speed [26].

Graph Neural Networks. Graph neural networks (GNNs) aggregate node characteristics through message-passing mechanisms and have gained widespread application in graph processing tasks [27]. GraphSAGE introduced inductive representation learning to enhance GNN performance on large-scale graphs [28]. Veličković *et al.* proposed the graph attention network (GAT), which employs attention mechanisms for more effective feature aggregation in graphs with complex interactions [29].

Representation Learning for Circuits. Representation learning enables models to capture the complex relationships between logic elements in circuits. FGNN and FGNN2 employed pre-training on circuit logic to significantly improve representation accuracy [11], [30]. DeepGate series also incorporated functional characteristics to generalize to complex circuits [12], [31], [32]. The circuit transformer maintained circuit equivalence to generate high-quality circuit representations [33], highlighting the potential of circuit representation learning. However, these methods often overlook critical ATPG-specific circuit states and fail to incorporate key features from ATPG, limiting their direct application to ATPG problems.

C. Machine Learning Applications in ATPG

Recently, machine learning techniques, particularly the combination of deep learning and RL, have offered new solutions for ATPG. Roy *et al.* proposed artificial neural networks to guide the decision-making process in ATPG [34]. SmartATPG used RL to automate test pattern generation [10]. HybMT proposed a machine learning algorithm based on a hybrid meta-predictor, which significantly improved test generation efficiency [35]. The application of reinforcement learning in ATPG has further demonstrated machine learning’s potential in improving test generation efficiency [10], [36].

However, as circuit size increases, these AI-guided methods still face challenges. Major issues include reward delay caused by long decision sequences and inadequate circuit state modeling, making RL model training and convergence more difficult and limiting their practical effectiveness in ATPG.

III. INF-ATPG FRAMEWORK

To address the aforementioned challenges introduced by existing solutions, we propose the InF-ATPG framework, which employs a novel RL-based approach utilizing block-level circuit search spaces and ATPG-specific circuit representations. Fig. 2

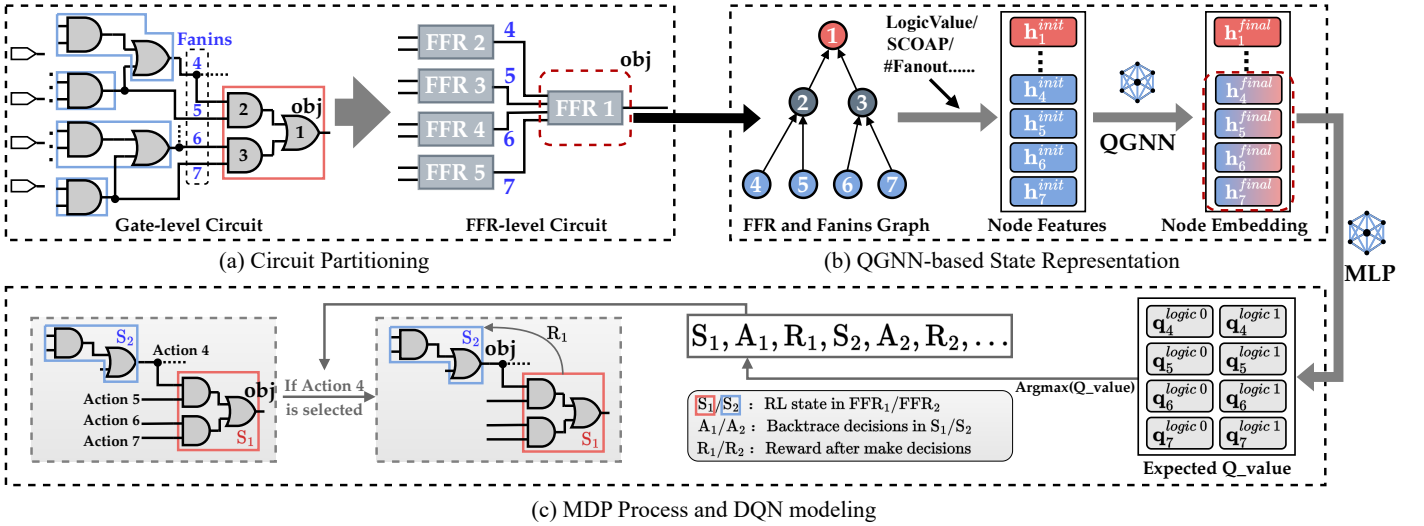


Fig. 2 Overview of the InF-ATPG framework. (a) Circuit partitioning into FFRs simplifies decision-making; (b) QGNN-based state representation improves the RL agent’s ability to generalize; (c) MDP and DQN modeling optimize test generation efficiency.

illustrates an overview of the InF-ATPG framework. Its key innovations are as follows:

- **Circuit partitioning and FFR backtrace (see Fig. 2(a)):** We first partition the circuit into Fanout-Free Regions (FFRs), which serve as the smallest decision-making units. This partitioning reduces the decision sequence length and mitigates reward delay by eliminating redundant decisions. Further details are provided in Section III-A.
- **QGNN-based state representation (see Fig. 2(b)):** While reducing decision length improves efficiency, it is essential to represent circuit states accurately to ensure correct decisions. To this end, we introduce a customized Quality-Value Graph Neural Network (QGNN) architecture, which captures critical features of FFR-based sub-circuits. QGNN enhances the RL agent’s generalization ability by learning complex relationships between circuit elements. Further details are discussed in Section III-B.
- **MDP process and DQN modeling (see Fig. 2(c)):** Building on the FFR partitioning and QGNN representation, we model the ATPG task as a Markov decision process (MDP). Key circuit state features are extracted, and a Deep Q-Network (DQN) is used to evaluate the action values of selecting different fanin gates within each FFR. Further elaboration on this aspect is provided in Section III-C.

A. Circuit Partitioning and FFR-Level Backtrace

Traditional ATPG algorithms encounter challenges such as long decision sequences and reward delay, particularly in large-scale circuits. To address these issues, the InF-ATPG framework adopts a partitioning strategy based on FFRs.

An FFR, a circuit sub-block with non-overlapping internal logic and a single output, encapsulates a self-contained unit of logic. This structure simplifies the decision-making process while providing a higher-level abstraction of the circuit by isolating the logic within the FFR. As shown in Fig. 3, FFR-level backtrace significantly reduces the decision sequence length

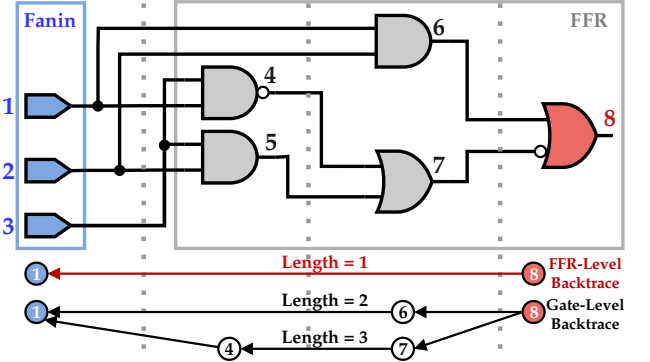


Fig. 3 Comparison of FFR-level and Gate-level backtrace. FFR-level backtrace shortens the decision sequence by directly targeting fanin gates, while Gate-level backtrace involves a longer sequence of intermediate gates.

compared to gate-level backtrace. The gate-level backtrace from the output gate 8 to the fanin gate 1 requires traversing multiple gates (i.e., gate 6, or gates 7 to 4), resulting in a longer decision sequence (length 2 or 3). In contrast, FFR-level backtrace directly targets the fanin gates of the FFR, reducing the sequence to a length of 1 by bypassing intermediate gates and directly focusing on the higher-level structure of the circuit.

By extracting each FFR in the circuit and its associated fanin gates to form a sub-circuit, InF-ATPG reduces the complexity of decision-making and solves the problem of reward delay. Each FFR becomes the smallest decision unit, allowing the framework to generate test patterns more efficiently than traditional gate-level approaches.

B. QGNN-based State Representation

In RL, accurately representing the logic state of circuits is a key challenge, especially when ATPG problems are modeled as partially observable Markov decision processes (POMDPs). The precision of state modeling directly impacts the general-

TABLE I Key circuit features in QGNN state representation

Feature	Description
Logic Value	The logic value of the node (i.e., 0, 1, X)
Objective Value	Expected logic value for objective gate (in PODEM)
SCOAP Controllability	Measures if the node can be controlled by PIs
SCOAP Observability	Measures if the node can be observed at a PO
Gate Type	One-hot encoded type of the logic gate
#Fanout	Number of fanout gates connected to the node
Depth	Depth of the node from the PIs

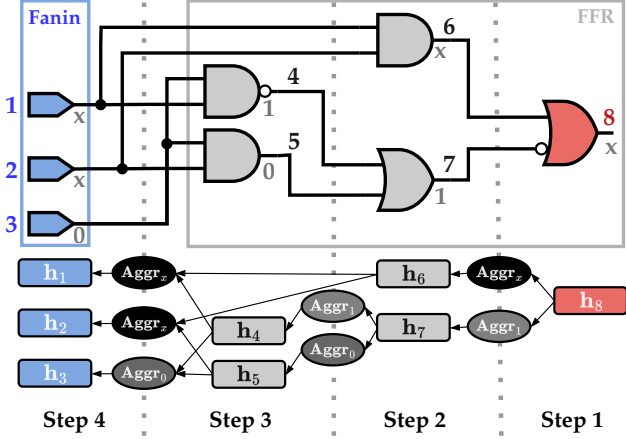


Fig. 4 QGNN aggregation process across different logic states in an FFR. Nodes with 0, 1, and X logic values use different aggregators to propagate information, enhancing the model’s ability to capture complex circuit dependencies.

ization ability of the RL model. Traditional ATPG methods primarily focus on individual gate characteristics, which limits their ability to capture complex circuit relationships, thereby affecting overall performance. To address this, the InF-ATPG framework introduces a customized quality-value graph neural network (QGNN) architecture. QGNN captures ATPG-specific features and introduces a logic-value-aware multi-aggregator design based on GAT [29], enabling a more precise representation of the action’s Q-value.

Circuit-Logic-State Features. QGNN utilizes a variety of key circuit features to construct a comprehensive state representation, as shown in TABLE I. The logic value directly reflects circuit functionality, while the objective value guides decision-making by adjusting targets. SCOAP controllability and observability quantify the difficulty of controlling and observing a node. These features capture both the static and dynamic characteristics of circuit states that are essential for ATPG, enabling QGNN to model essential circuit logic states more effectively than heuristic methods. QGNN generates a more robust state representation, significantly enhancing the RL agent’s ability to make optimal decisions during ATPG.

QGNN Model. QGNN models each FFR and its fanin gates as a graph, where each logic gate is represented as a node, and edges represent the connections between gates. As illustrated in Fig. 4, the model assigns an embedding vector (e.g., h_1, h_2, h_3) to each node, encoding its features. These embeddings are then updated through message aggregating and passing using a GAT, which aggregates information in the reverse direction of

circuit computation, layer by layer. The aggregation process is governed by the following equations:

$$\begin{aligned} \alpha_{ij} &= \text{softmax}_j((\mathbf{W}_q \mathbf{h}_i)^\top \cdot (\mathbf{W}_k \mathbf{h}_j)), \\ \mathbf{m}_j &= \mathbf{W}_v \mathbf{h}_j, \\ \text{msg}_i &= \text{aggr}(\mathbf{h}_j \mid j \in P(i)) = \sum_{j \in P(i)} (\alpha_{ij} \cdot \mathbf{m}_j), \end{aligned} \quad (1)$$

where $P(i)$ represents the predecessors of node i , α_{ij} represents the attention weight between node i and node j , and $\mathbf{W}_q, \mathbf{W}_k, \mathbf{W}_v$ are the weight matrices of the aggregator. The aggregated message msg_i is then passed to a gated recurrent unit (GRU) to update the node’s embedding:

$$\mathbf{h}_i \leftarrow \text{GRU}(\mathbf{h}_i, \text{aggr}(\mathbf{h}_j \mid j \in P(i))). \quad (2)$$

This process allows QGNN to capture the complex dependencies between nodes in the circuit, ultimately producing final embeddings for the target FFR. These embeddings provide rich information for the RL agent to select optimal actions during ATPG.

Innovative Aggregator Design. One of the key innovations in QGNN is the use of multiple aggregators tailored to different logic states (0, 1, X). As shown in Fig. 4, different aggregators ($\text{aggr}_0, \text{aggr}_1, \text{aggr}_X$) are applied depending on the logic value of the node. This design ensures that the information flow is adapted to the specific logic state of each node, allowing for more precise information propagation. The aggregation functions for different logic states are defined as follows:

$$\begin{aligned} 0\text{-aggr} &\rightarrow \text{GRU}_{\text{logic}0}(\mathbf{h}_i, \text{aggr}_{\text{logic}0}(\mathbf{h}_j \mid j \in P(i))), \\ 1\text{-aggr} &\rightarrow \text{GRU}_{\text{logic}1}(\mathbf{h}_i, \text{aggr}_{\text{logic}1}(\mathbf{h}_j \mid j \in P(i))), \\ X\text{-aggr} &\rightarrow \text{GRU}_{\text{logic}X}(\mathbf{h}_i, \text{aggr}_{\text{logic}X}(\mathbf{h}_j \mid j \in P(i))). \end{aligned} \quad (3)$$

This design is critical because nodes with different logic values (i.e., 0, 1, X) often exhibit different signal propagation behaviors. By decoupling the aggregation processes for different logic states, QGNN ensures that the information relevant to each state is processed independently, improving the expressiveness of the model.

C. MDP and DQN Modeling

Building on FFR partitioning and QGNN-based state representation, the InF-ATPG framework models the ATPG problem as an MDP and incorporates a tailored DQN framework to train the QGNN-driven RL agent for optimal action selection.

MDP Modeling. To enable the RL agent to navigate the complexities of circuit testing effectively, the key elements of the MDP include:

- **State:** The state is defined by the logic state and circuit features of each FFR. The QGNN generates embedding vectors that represent the state of each FFR in the circuit.
- **Action:** Based on the QGNN state embeddings, the RL agent selects actions, which involve choosing a fanin gate in each FFR for the backtrace process. The action space is unified across FFRs regardless of the number of fanins.
- **Reward:** The reward function is designed to reduce backtracks and prioritize critical primary inputs (PIs), thereby

accelerating test generation. ①The reward function penalizes unnecessary decisions with a small negative reward (-0.1). ②When reaching a PI, the reward function assigns rewards based on the frequency of this PI’s visits and the number of backtracks encountered between assigning a value to this PI and the next backtrack step. By this, we impose immediate penalties on conflicting PIs and avoid redundant visits. ③If a test is successfully generated or the backtrack limit is exceeded, the episode ends with a corresponding reward, thereby aligning the training process with the objective of test generation:

$$\text{Reward} = \begin{cases} -0.1, & \text{if not reach PI;} \\ 10 - \lambda_1 \cdot e^{\lambda_2 \cdot N}, & \text{if reach PI;} \\ 100, & \text{Test found/No test;} \\ -100, & \text{Over backtrack limit;} \end{cases}$$

$$N = \#\text{backtracks}[\text{PI}] + \#\text{visits}[\text{PI}].$$

DQN Modeling. The DQN process is illustrated in Fig. 5, and the key steps are as follows:

- **Action Value Evaluation:** To enhance the effectiveness of circuit representation in RL-driven test generation, InF-ATPG employs the constructed QGNN alongside a multilayer perceptron (MLP) as the value network to guide the RL agent. This value network predicts the future value of all possible actions, with the action carrying the highest Q-value selected as the optimal choice.
- **Q-Value Update:** The QGNN and MLP are updated to minimize the loss between the predicted Q-values and the Q-targets. The Q-targets are computed using the target QGNN and target MLP, which is periodically updated.
- **Exploration-Exploitation Trade-off:** During training, exploration selects actions randomly to ensure the model explores diverse possibilities, while exploitation chooses actions based on the highest Q-value to optimize decision-making. The exploration rate starts high to encourage broad exploration and is gradually reduced as training progresses, shifting the model towards exploitation for more refined, optimal strategies.

The training process leverages a prioritized experience replay (PER) buffer, where transitions (state, action, reward, next state, done) are stored during interaction with the circuit environment. Over time, the DQN samples transition from the PER buffer to learn and update. The QGNN and MLP are continuously updated based on the loss, ensuring the RL agent improves its decision-making over time.

IV. EXPERIMENTAL RESULTS

A. Experimental Setup

All experiments were performed on NVIDIA A100 GPU and Intel Xeon Processor (Skylake, IBRS) @ 2.99GHz, running Ubuntu 20.04. The primary goal was to evaluate the performance of InF-ATPG in comparison to the traditional ATPG method and the unimproved GNN-based approach. As baseline methods, we used a standard PODEM based on gate-level heuristic [37], an improved PODEM based on FFR-level

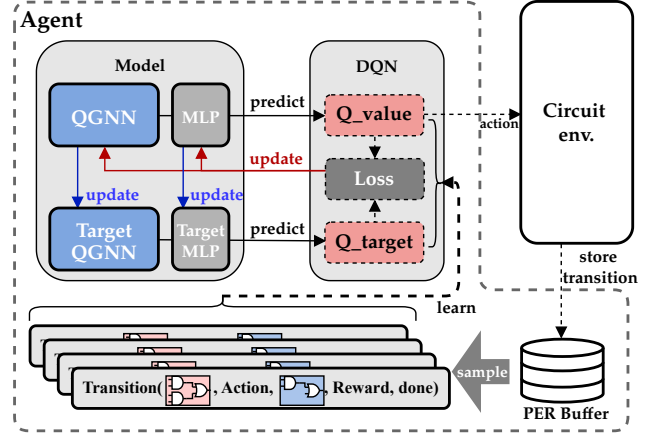


Fig. 5 MDP and DQN process in InF-ATPG. The QGNN generates state embeddings, and the DQN evaluates action values, selects actions, and updates the model through reinforcement learning. Transitions are stored and sampled from a PER buffer to optimize learning efficiency.

heuristic, and an FFR-level GNN approach without the QGNN enhancements introduced in our framework.

Benchmark circuits from the ISCAS-85 [38] and ISCAS-89 [39] suites were selected to cover a range of circuit sizes and complexities, from 607 gates (*c432*) to 19,768 gates (*s38417*). It is noteworthy that the benchmark circuits were synthesized from RTL code and fault injection was performed using the oATPG [37] fault injection algorithm (oATPG [37] inserts faults at the pins of each cell to comply with industrial-grade ATPG workflows). Consequently, these benchmarks differ from the standard ISCAS-85 and ISCAS-89 benchmarks in both circuits and faults.

For hyperparameters, the QGNN and MLP learning rate were set to 0.0001, with a discount factor γ of 0.95. The capacity of the PER buffer was configured as 512×1024 . Through extensive experimental exploration and parameter sensitivity analysis, the reward function parameters λ_1 and λ_2 were ultimately determined to be 7.5 and 0.07. To ensure fairness and consistency, all comparison methods were evaluated under identical experimental conditions.

For training, we selected 100 challenging faults from each circuit and conducted 10 training epochs. The remaining faults were used as the test set, allowing us to rigorously evaluate the generalization and effectiveness of the InF-ATPG framework. Due to differences in implementation languages—InF-ATPG being a Python/C++ hybrid and the open-source gate-level ATPG heuristic [37] implemented in C++—a direct comparison of CPU time would be unfair. Therefore, when comparing InF-ATPG with other baselines, we exclusively use the number of backtracks as a proxy metric to evaluate ATPG performance. Conversely, we directly compare the CPU runtime improvements of heuristic-based FFR-level ATPG versus Gate-level ATPG. By examining both the reduction in the number of backtracks between InF-ATPG and other methods, and the CPU runtime reduction between FFR-level ATPG and Gate-level ATPG, we can demonstrate that InF-ATPG has potential

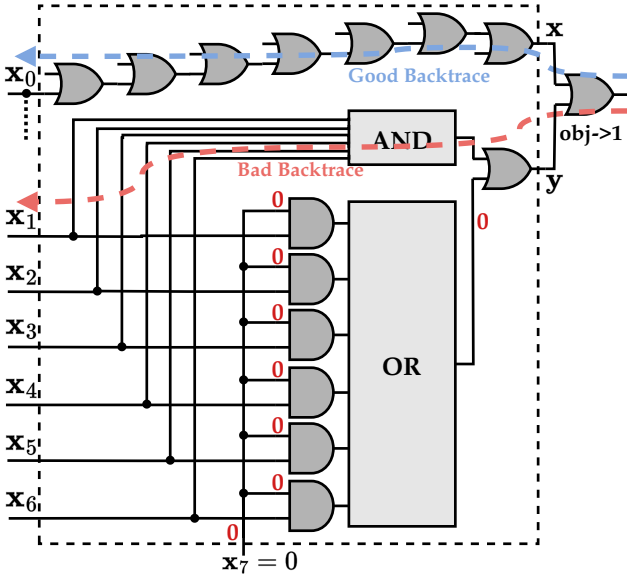


Fig. 6 Gate-level decision-making, constrained by single-gate information, results in suboptimal backtrack decisions. In this instance, with x_7 assigned to 0, setting gate y to logic 1 would require all inputs x_1 - x_6 to be 1. Conversely, FFR-level decision-making can identify that a single backtrack through gate x efficiently achieves the objective gate’s target.

to achieve superior results through AI methods based on FFR-level decision-making.

B. Experimental Results and Analysis

This section presents a concise analysis of the experimental results focused on backtrack reduction and fault coverage improvement. Additionally, we conducted experiments to further validate our method’s effectiveness by demonstrating the CPU runtime reduction of FFR-level compared to Gate-level approaches, as well as the decision sequence length reduction of InF-ATPG relative to Gate-level approaches. We compare InF-ATPG with gate-level and FFR-level ATPG approaches, and include an ablation study to highlight the contributions of key components.

Backtrack and Backtrace Reduction. As shown in the upper part of TABLE II, InF-ATPG achieves a significant reduction in backtracks and backtrack steps in various circuits when controlling for different methods to achieve the same fault coverage. On average, InF-ATPG reduces backtracks by 55.06% compared to gate-level heuristic ATPG [37] and by 52.21% compared to FFR-level heuristic ATPG. Moreover, compared to FFR-level GNN without QGNN enhancements, InF-ATPG reduces backtracks by 38.31% and backtrack steps by 38.38%. The consistent improvements across different circuits underscore the robustness of the proposed method.

The FFR-based partitioning strategy simplifies decision-making by dividing circuits into smaller, independent sub-blocks, reducing decision sequence length and minimizing backtracks for ATPG. Additionally, the QGNN-enhanced state representation provides the RL agent with more accurate circuit information, enabling more informed decisions. This highlights

InF-ATPG’s ability to significantly reduce computational complexity, especially for large-scale circuits.

Fault Detection and Coverage. As presented in the lower section of TABLE II, under the same max-backtrack limit, InF-ATPG successfully detects hard-to-detect faults that other methods fail to detect. InF-ATPG achieves an average undetected fault percentage (UFP) of 0.50%. This represents a 30.32% improvement compared to gate-level heuristic ATPG [37], which has a UFP of 0.62%, and a 42.64% improvement over FFR-level heuristic ATPG, which has a UFP of 0.73%.

While the average improvement is notable, InF-ATPG shows particularly significant gains on larger circuits, such as *s9234* and *s15850*, where undetected faults were reduced by over 90% compared to other methods. These improvements are attributed to the QGNN-based state representation, which captures deeper circuit features, allowing RL agent to optimize test generation.

CPU Runtime. As illustrated in TABLE III, this experiment aims to demonstrate that although both approaches utilize distance-based heuristic methods, decision-making at the FFR-level yields superior results compared to Gate-level decision-making. Table 3 reveals that for larger-scale circuits, FFR-level decision-making contributes to a reduction in CPU runtime. For instance, in the *s38417* circuit, FFR-level decision-making reduced runtime by 39.20% compared to the Gate-level approach [37]. Conversely, TABLE III indicates that for smaller-scale circuits, FFR-level decision-making incurs significant initialization overhead due to the computational requirements of FFR calculation, thus requiring longer CPU time compared to the Gate-level approach [37].

FFR-level decision-making provides a broader perspective compared to Gate-level decision-making. As exemplified in Fig. 6, to set the objective gate to logic 1, Gate-level decision-making tends to select gate y with smaller logic depth. However, in this example, since x_7 has already been assigned a value of 0, adjusting gate y to 1 incurs a substantial cost (requiring x_1 - x_6 all to be set to 1). Consequently, selecting gate y for backtrack is not an optimal choice. In contrast, FFR-level decision-making has the opportunity to comprehensively consider the logical state and topological connectivity relationships at the subcircuit level, thereby recognizing that performing a backtrack through gate x can achieve the objective gate’s target more efficiently.

Decision Sequence Length Reduction. This experiment was designed to demonstrate the respective impacts of FFR and QGNN on reducing the decision sequence length. TABLE IV shows that InF-ATPG reduces decision sequence length by an average factor of 7.0 compared to gate-level ATPG [37], with a notable reduction of 15.7 in the case of *s9234*.

This reduction stems from the FFR partitioning strategy, which simplifies the decision process by dividing the circuit into smaller, independent regions, each with an average FFR depth of 5.2. This coarse-grained approach reduces the complexity of decision sequences by focusing on broader, higher-level sub-circuits. Also, InF-ATPG achieves an average reduction of 7.0, which surpasses the average FFR depth of 5.2. Guided by QGNN’s enriched state representation, the RL

TABLE II Comprehensive Performance Comparison of InF-ATPG with Gate-level and FFR-level ATPG Approaches

Circuit	#Gates	InF-ATPG		Gate-level [37]				FFR-level heuristic				FFR-level GNN			
		#B-track	#B-trace	#B-track	Red1(%)	#B-trace	Red2(%)	#B-track	Red1(%)	#B-trace	Red2(%)	#B-track	Red1(%)	#B-trace	Red2(%)
c432	607	27017	39417	46422	41.80	50809	22.42	41458	34.83	46165	14.62	47447	43.06	51587	23.59
c1908	1514	8414	10903	14617	42.44	22568	51.69	13058	35.56	21654	49.65	11372	26.01	19264	43.40
c1355	1792	19519	35861	47679	59.06	63557	43.58	118609	83.54	133023	73.04	55033	64.53	68635	47.75
c2670	2335	37277	41753	41222	9.57	60486	30.97	32979	-13.03	46616	10.43	29301	-27.22	44949	7.11
c3540	3080	32374	40576	72348	55.25	83859	51.61	96705	66.52	107593	62.29	64676	49.94	73104	44.50
s9234	3518	5406	19909	75294	92.82	90508	78.00	82638	93.46	100165	80.12	10623	49.11	24620	19.13
s15850	7290	10295	10295	51085	79.85	69527	85.19	43268	76.21	61271	83.20	24861	58.59	42603	75.84
s38417	19768	53341	79765	132197	59.65	185653	57.04	89792	40.59	136154	41.42	92706	42.46	146852	45.68
Average	-	-	-	-	55.06	-	52.56	-	52.21	-	51.85	-	38.31	-	38.38

Circuit	#Faults	InF-ATPG		Gate-level [37]			FFR-level heuristic				FFR-level GNN				
		#UD-Fault	UFP(%)	#UD-Fault	Diff.(#)	UFP(%)	Imp.(%)	#UD-Fault	Diff.(#)	UFP(%)	Imp.(%)	#UD-Fault	Diff.(#)	UFP(%)	Imp.(%)
c432	1740	20	1.15	20	0	1.15	0.0	20	0	1.15	0.0	20	0	1.15	0.0
c1908	4284	9	0.21	9	0	0.21	0.0	11	2	0.26	18.18	9	0	0.21	0.0
c1355	4932	3	0.06	3	0	0.06	0.0	41	38	0.83	92.68	4	1	0.08	25.00
c2670	6250	107	1.71	107	0	1.71	0.0	107	0	1.71	0.0	107	0	1.71	0.0
c3540	8710	63	0.72	66	3	0.76	4.54	72	9	0.83	12.50	63	0	0.72	0.0
s9234	6396	4	0.06	39	35	0.61	89.74	42	38	0.66	90.48	4	0	0.06	0.0
s15850	13294	4	0.03	50	46	0.38	92.00	46	42	0.35	91.30	7	3	0.05	42.86
s38417	36786	16	0.04	36	20	0.10	55.55	25	9	0.07	36.00	27	11	0.07	40.74
Average	-	-	0.50	-	+13	0.62	30.23	-	+17	0.73	42.64	-	+2	0.51	13.58

- Gate-level [37]: Gate-level PODEM algorithm using a distance-from-primary-inputs heuristic.
- FFR-level heuristic: FFR-level PODEM algorithm using a distance-from-primary-inputs heuristic.
- FFR-level GNN: FFR-level ATPG approach that utilizes unimproved GNN (without QGNN), enhancing with RL.
- #B-track: The total number of backtracks performed during ATPG.
- #B-trace: The total backtrack steps during ATPG refer to the process of tracing from the objective gate to PI.
- #UD-Fault: Undetected faults number in the method. UFP(%): Undetected faults percentage to total faults in the method.
- Red1/Red2 (%): Percentage reduction in the number of backtracks (Red1) and backtrack steps (Red2) compared to this method. Positive values indicate that the InF-ATPG approach achieved fewer backtracks and backtrack steps.
- Diff. (#)/Imp. (%): The difference in the number of undetected faults (Diff.) and the improvement in UFP (Imp.) compared to this method. Positive values indicate a reduction in undetected faults and an improvement in UFP.

TABLE III CPU time comparison between FFR-level and gate-level ATPG

Circuit	FFR-level(ms)	Gate-level [37](ms)	CPU Time Red.(%)
c432	221	117	-88.89
c1908	112	91	-23.07
c1355	705	243	-190.12
c2670	221	209	-5.74
c3540	1008	1028	1.95
s9234	441	495	10.91
s15850	695	731	4.92
s38417	1629	2667	39.20

- CPU Time Red.(%): Reduction of CPU time by FFR-level ATPG, calculated as (Gate-level-FFR-level) / (Gate-level).

agent leverages this broader context to make more informed decisions, reducing unnecessary steps, and further improving efficiency. This combination of coarse-grained partitioning and enhanced decision-making allows InF-ATPG to significantly shorten decision sequences, making it scalable for larger circuits.

The results confirm that InF-ATPG substantially reduces backtracks, enhances fault coverage, and shortens decision sequences. The ablation study underscores the critical role of FFR partitioning in reducing decision complexity, the effectiveness of QGNN-based state representation in capturing circuit logic for improved fault detection, and the contribution of RL in optimizing decision-making.

TABLE IV Decision sequence length comparison between InF-ATPG and gate-level ATPG

Circuit	FFR Avg-Dep.	InF-ATPG	Gate-level [37]	Ratio (×)
c432	5.0	119234	1169414	9.8
c1908	5.9	89363	549736	6.2
c1355	8.2	335034	1844036	5.5
c2670	4.8	173617	700113	4.0
c3540	6.2	289443	2371960	8.2
s9234	3.7	70286	1104367	15.7
s15850	3.5	70669	645829	9.1
s38417	3.9	266244	1521569	5.7
Average	5.2	176736	1238378	7.0

- FFR Avg-Dep.: Average depth of FFRs in the circuit.
- Ratio (×): Reduction of decision sequence length by InF-ATPG, calculated as (Gate-level) / (InF-ATPG).

V. CONCLUSION AND FUTURE WORK

In this paper, we introduce InF-ATPG, a novel RL-based ATPG approach that leverages block-level circuit search spaces and advanced ATPG-specific circuit representations. By modeling circuits at the FFR level, we effectively reduce the decision sequence length, thereby addressing the reward delay issues commonly encountered in RL models. Furthermore, integrating key circuit features into the QGNN framework enhances the representation of circuit states and functionalities by decoupling the aggregation processes for different logic states. Experimental results demonstrate a 55.06% reduction in backtracks

compared to the traditional gate-level method and a 38.31% reduction over the unimproved machine learning approach.

Future work could investigate the integration of more sophisticated reinforcement learning algorithms and additional circuit characteristics to further enhance the efficiency and accuracy of the ATPG process. Moreover, exploring efficient deployment strategies for these models within existing ATPG frameworks represents a compelling research direction that could significantly advance the practical applicability of AI-guided ATPG methods in industrial settings.

REFERENCES

- [1] J.-G. Jang, "On a design and implementation technique of a universal atpg for vlsi circuits," *The Transactions of the Korea Information Processing Society*, vol. 2, no. 3, pp. 425–432, 1995.
- [2] C. Barnhart, V. Brunkhorst, F. Distler, O. Farnsworth, B. Keller, and B. Koenemann, "Opmisr: The foundation for compressed atpg vectors," in *Proceedings International Test Conference 2001 (Cat. No. 01CH37260)*. IEEE, 2001, pp. 748–757.
- [3] L. Lavagno, I. L. Markov, G. Martin, and L. K. Scheffer, *Electronic design automation for IC system design, verification, and testing*. CRC Press, 2017.
- [4] K. Y. Kamal, "The silicon age: Trends in semiconductor devices industry," *Journal of Engineering Science & Technology Review*, vol. 15, no. 1, 2022.
- [5] H.-L. Zhen, N. Wang, J. Huang, X. Huang, M. Yuan, and Y. Huang, "Conflict-driven structural learning towards higher coverage rate in atpg," *arXiv preprint arXiv:2303.02290*, 2023.
- [6] L.-T. Wang, C.-W. Wu, and X. Wen, *VLSI test principles and architectures: design for testability*. Elsevier, 2006.
- [7] W. Kunz, J. Marques-Silva, and S. Malik, "Sat and atpg: Algorithms for boolean decision problems," in *Logic synthesis and Verification*. Springer, 2002, pp. 309–341.
- [8] M. Bushnell and V. Agrawal, *Essentials of electronic testing for digital, memory and mixed-signal VLSI circuits*. Springer Science & Business Media, 2004, vol. 17.
- [9] H. Chen and J. Marques-Silva, "A two-variable model for sat-based atpg," *IEEE Transactions on Computer-Aided Design of Integrated Circuits and Systems*, vol. 32, no. 12, pp. 1943–1956, 2013.
- [10] W. Li, H. Lyu, S. Liang, T. Wang, and H. Li, "Smartatpg: Learning-based automatic test pattern generation with graph convolutional network and reinforcement learning," in *Proceedings of the 61st ACM/IEEE Design Automation Conference*, 2024, pp. 1–6.
- [11] Z. Wang, C. Bai, Z. He, G. Zhang, Q. Xu, T.-Y. Ho, Y. Huang, and B. Yu, "Fgmn2: A powerful pre-training framework for learning the logic functionality of circuits," *IEEE Transactions on Computer-Aided Design of Integrated Circuits and Systems*, 2024.
- [12] Z. Shi, H. Pan, S. Khan, M. Li, Y. Liu, J. Huang, H.-L. Zhen, M. Yuan, Z. Chu, and Q. Xu, "Deepgate2: Functionality-aware circuit representation learning," in *2023 IEEE/ACM International Conference on Computer Aided Design (ICCAD)*. IEEE, 2023, pp. 1–9.
- [13] L. Goldstein, "Controllability/observability analysis of digital circuits," *IEEE Transactions on Circuits and Systems*, vol. 26, no. 9, pp. 685–693, 1979.
- [14] J. Cong, Z. Li, and R. Bagrodia, "Acyclic multi-way partitioning of boolean networks," in *Proceedings of the 31st annual design automation conference*, 1994, pp. 670–675.
- [15] J. P. Roth, "Diagnosis of automata failures: A calculus and a method," *IBM journal of Research and Development*, vol. 10, no. 4, pp. 278–291, 1966.
- [16] Goel, "An implicit enumeration algorithm to generate tests for combinational logic circuits," *IEEE transactions on Computers*, vol. 100, no. 3, pp. 215–222, 1981.
- [17] Fujiwara and Shimono, "On the acceleration of test generation algorithms," *IEEE Transactions on Computers*, vol. 100, no. 12, pp. 1137–1144, 1983.
- [18] T. Larrabee, "Test pattern generation using boolean satisfiability," *IEEE Transactions on Computer-Aided Design of Integrated Circuits and Systems*, vol. 11, no. 1, pp. 4–15, 1992.
- [19] J. Huang, H.-L. Zhen, N. Wang, H. Mao, M. Yuan, and Y. Huang, "Neural fault analysis for sat-based atpg," in *2022 IEEE International Test Conference (ITC)*. IEEE, 2022, pp. 36–45.
- [20] R. Drechsler, S. Eggergluss, G. Fey, A. Glowatz, F. Hapke, J. Schloeffel, and D. Tille, "On acceleration of sat-based atpg for industrial designs," *IEEE Transactions on Computer-Aided Design of Integrated Circuits and Systems*, vol. 27, no. 7, pp. 1329–1333, 2008.
- [21] S. Bandyopadhyay, S. K. Pal, and C. Murthy, "Simulated annealing based pattern classification," *Information Sciences*, vol. 109, no. 1-4, pp. 165–184, 1998.
- [22] F. Corno, P. Prinetto, M. Rebaudenpgo, and M. S. Reorda, "Saara: a simulated annealing algorithm for test pattern generation for digital circuits," in *Proceedings of the 1997 ACM symposium on Applied computing*, 1997, pp. 228–232.
- [23] R. S. Sutton, "Reinforcement learning, a bradford book," (*No Title*), 1998.

- [24] C. J. Watkins and P. Dayan, "Q-learning," *Machine learning*, vol. 8, pp. 279–292, 1992.
- [25] V. Mnih, "Playing atari with deep reinforcement learning," *arXiv preprint arXiv:1312.5602*, 2013.
- [26] T. Schaul, "Prioritized experience replay," *arXiv preprint arXiv:1511.05952*, 2015.
- [27] M. Niepert, M. Ahmed, and K. Kutzkov, "Learning convolutional neural networks for graphs," in *International conference on machine learning*. PMLR, 2016, pp. 2014–2023.
- [28] W. Hamilton, Z. Ying, and J. Leskovec, "Inductive representation learning on large graphs," *Advances in neural information processing systems*, vol. 30, 2017.
- [29] P. Velickovic, G. Cucurull, A. Casanova, A. Romero, P. Lio, Y. Bengio *et al.*, "Graph attention networks," *stat*, vol. 1050, no. 20, pp. 10–48 550, 2017.
- [30] Z. Wang, C. Bai, Z. He, G. Zhang, Q. Xu, T.-Y. Ho, B. Yu, and Y. Huang, "Functionality matters in netlist representation learning," in *Proceedings of the 59th ACM/IEEE Design Automation Conference, 2022*, pp. 61–66.
- [31] M. Li, S. Khan, Z. Shi, N. Wang, H. Yu, and Q. Xu, "Deepgate: Learning neural representations of logic gates," in *Proceedings of the 59th ACM/IEEE Design Automation Conference, 2022*, pp. 667–672.
- [32] Z. Shi, Z. Zheng, S. Khan, J. Zhong, M. Li, and Q. Xu, "Deepgate3: Towards scalable circuit representation learning," *arXiv preprint arXiv:2407.11095*, 2024.
- [33] X. Li, X. Li, L. Chen, X. Zhang, M. Yuan, and J. Wang, "Circuit transformer: A transformer that preserves logical equivalence."
- [34] S. Roy, S. K. Millican, and V. D. Agrawal, "Machine intelligence for efficient test pattern generation," in *2020 IEEE International Test Conference (ITC)*. IEEE, 2020, pp. 1–5.
- [35] S. P. J. S. R. Sarangi, "Hybmt: Hybrid meta-predictor based ml algorithm for fast test vector generation."
- [36] W. Li, H. Lyu, S. Liang, T. Wang, P. Tian, and H. Li, "Intelligent automatic test pattern generation for digital circuits based on reinforcement learning," in *2023 IEEE 32nd Asian Test Symposium (ATS)*. IEEE, 2023, pp. 1–6.
- [37] "oATPG," 2022, [Online]. Available: <https://www.gitlink.org.cn/opensdacs/oCASatpg/>.
- [38] F. Brglez, "A neutral netlist of 10 combinational benchmark circuits and a target simulator in fortran," in *International Symposium on Circuits and Systems, 1985*, 1985, pp. 695–698.
- [39] F. Brglez, D. Bryan, and K. Kozminski, "Combinational profiles of sequential benchmark circuits," in *1989 IEEE International Symposium on Circuits and Systems (ISCAS)*. IEEE, 1989, pp. 1929–1934.